HOSTED BY
ELSEVIER
CrossMark
Available online at www.sciencedirect.com
ScienceDirect
Progress in Natural Science: Materials International 24 (2014) 539–546
Progress in Natural Science Materials International
www.elsevier.com/locate/pnsmi
www.sciencedirect.com

Original Research

Corrosion of magnesium and magnesium–calcium alloy in biologically-simulated environment

Richard Harrison[b], Diana Maradze[a], Simon Lyons[a], Yufeng Zheng[c], Yang Liu[a,*]

[a]*Wolfson School of Mechanical and Manufacturing Engineering, Loughborough University, Loughborough, Leicestershire LE11 3TU, UK*
[b]*Wolfson Centre for Stem Cells, Tissue Engineering and Modelling (STEM), Centre for Biomolecular Sciences, University of Nottingham, Nottingham NG7 2RD, UK*
[c]*College of Engineering, Peking University, Beijing 100871, China*

Received 2 July 2014; accepted 1 September 2014
Available online 29 October 2014

Abstract

A study of biocompatibility and corrosion of both metallic magnesium (Mg) and a magnesium alloy containing 1% calcium (Mg–Ca) were investigated in *in vitro* culture conditions with and without the presence of bone marrow derived human mesenchymal stem cells (hMSCs). Chemical analysis of the degraded samples was performed using XRD and FEGSEM. The results from the XRD analysis strongly suggested that crystalline phase of magnesium carbonate was present on the surface of both the Mg and Mg–Ca samples. Flame absorption spectrometry was used to analyse the release of magnesium and calcium ions into the cell culture medium. Magnesium concentration was kept consistently at a level ranging from 40 to 80 mM for both Mg and Mg–Ca samples. No cell growth was observed when in direct contact with the metals apart from a few cells observed at the bottom of culture plate containing Mg–Ca alloy. In general, *in vitro* study of corrosion of Mg–Ca in a biologically-simulated environment using cell culture medium with the presence of hMSCs demonstrated close resemblances to *in vivo* corrosion. Although *in vitro* corrosion of Mg–Ca revealed slow corrosion rate and no immediate cytotoxicity effects to hMSCs, its corrosion rate was still too high to achieve normal stem cell growth when cells and alloys were cultured *in vitro* in direct contact.

Keywords: Magnesium; Biometal; Corrosion; Biocompatibility; Stem cells; *In vitro*

1. Introduction

Due to the limitations associated with the current methods better material for orthopaedic implantation is required and researchers have been studying the use of biodegradable magnesium alloy as a candidate for orthopaedic implantation. Of the metals currently employed as biomaterials, magnesium alloys thereof demonstrate an excellent load bearing profile with an elastic modulus of 41–45 GPa which is much closer to cortical bone tissue (20 GPa) than most common metal biomaterials [1–4]. This is further facilitated by increased osseointegration of the magnesium with bone tissue [5]. When combined, these factors reduce the potential for stress shielding and hence, the incidence of implant failure. Furthermore, magnesium structures readily degrade *in vivo* allowing the implant to act only as an aid to biological repair, becoming less important as the requirement for support lessens. In addition, magnesium ion also has a number of important biological functions, including taking part in bone and mineral homoeostasis [6–8] promoting DNA replication and transcription [7,9] and regulation of opening and closing of ion channels [7,8,10–12]. Magnesium normal physiological range is between 0.8 mM and 1.0 mM, approximately 60–65% is stored in the bone and homoeostasis is maintained by the kidneys and intestine [13].

During fracture healing the biomaterial implant should have the ability to sustain mechanical strength until the formation of new bone bridges the gap of the fracture. In order for this to happen the biodegradable material should degrade gradually to allow for tissue implant integration. Pure magnesium has a high corrosion rate in physiological environment; this is a major limitation as the implant corrodes faster than new bone

*Corresponding author. Tel.: +44 1509 227602; fax: +44 1509 227648.
E-mail address: Y.Liu3@lboro.ac.uk (Y. Liu).
Peer review under responsibility of Chinese Materials Research Society.

http://dx.doi.org/10.1016/j.pnsc.2014.08.010
1002-0071/

formation [14–17]. When pure magnesium is placed in aqueous environment, magnesium reacts with water to form magnesium hydroxide and hydrogen gas. The hydroxide film provides some protection to further corrosion and exposure of magnesium to chloride ions results in pitting corrosion which in turn could lead to implant failure [18]. Furthermore cells are sensitive to the corrosion environment created by the corrosion of magnesium [19,20].

Research has shown that corrosion resistance of magnesium implants can be improved through alloying and surface coating. The use of hydroxyapatite for surface coating has been shown to reduce corrosion rate of magnesium and magnesium alloys [16,20,21], and to have osteo-conductive properties [22]. A number of alloying elements have been studied for magnesium-based implants; these include aluminium, zinc, calcium, yttrium and rare earths. Studies have shown that alloying results in increased implant strength, reduced corrosion rate [14,16,23,24], and slower release of magnesium ions into the medium [19]. Magnesium implants alloyed with calcium or zinc or both show improved cell viability, stability in physiological conditions and enhanced cell attachment and proliferation [14,24,25]. When examining the corrosion of a magnesium alloy for biological applications two broad factors, the corrosion behaviour of magnesium, and the interaction and toxicity of magnesium to local tissue, must be considered [2]. Hence, one of the major challenges faced in the development of magnesium based biomaterials is how to predict the corrosion process and the corresponding biological and physiological consequence of such corrosion in the context of implants and implantation sites. The biodegradability of magnesium through corrosion is a double-edged sword and it is just this particular nature that cause concerns on applying standard approach to *in vitro* biocompatibility and corrosion test.

In previous studies [24], a much faster corrosion rate of Mg–Ca alloy implant was observed in *in vitro* electrochemical test compared to those observed *in vivo*. Also high activity of osteoblast and circumferential osteogenesis were observed around the Mg–Ca alloy pin *in vivo*, but still an unfilled void was left at implantation site when the Mg pin was totally degraded at the end of the 3 month implantation. Thus, there is a lack of correlation of *in vitro* and *in vivo* corrosion study and, as well, of understanding the effects of Mg corrosion products on stem cells responsible for bone tissue regeneration [24]. Here we present study on the biocompatibility and corrosion of magnesium containing 1% calcium in the presence and absence of bone marrow derived human mesenchymal stem cells, aiming to mimic the *in vivo* environment at the implantation sites.

2. Materials and methods

2.1. Mg sample preparation

Commercial pure magnesium (99.9%) and magnesium–1% calcium were prepared in the form of cylindrical ingots, and treated and cleaned as described previously [24]. The magnesium ingots were then cut into disks and sterilised using ethanol and UV light. Mg disks had average measurements of 12.2 mm diameter and 4.75 mm depth. Mg–Ca disks had average measurements of 16.23 mm diameter and 3.37 mm depth. Average surface areas were 415.85 mm^2 per disk for Mg and 582.7 mm^2 for Mg–Ca. This allowed a correctional factor of 1.4 to be applied to the data to compensate for the lower surface area of the Mg disks.

2.2. Cell culture

hMSC (Lonza, UK) were used for experimental procedures. Cells were cultured in growth medium Dulbecco's Modified Eagle's Medium (Lonza, UK) supplemented with 10% (v/v) foetal calf serum (FCS) (Sigma-Aldrich, UK), L-glutamine final media concentration 2 mM (Sigma-Aldrich, UK), and 100 units/ml antibiotic–antimycotic (Sigma-Aldrich, UK).

2.3. In vitro corrosion with/without the cell presence

Samples were incubated for 11 days in cell culture medium at 37 °C 5% CO_2. Samples where either incubated in cell culture medium with or without the presence of cells to evaluate the effect of cells on magnesium alloy corrosion behaviour. Cells were seeded at a seeding density of 1.5×10^5 cells/well in a six well plate. 1 ml of conditioned medium was collected every 24 hrs and replaced with 1 ml of fresh medium. The conditioned medium collected was kept frozen for further analysis. Cells seeded in each well were fixed in 70% methanol in distilled water for 25 mins. These were then washed and stored in PBS (Sigma-Aldrich, UK). Assessment of cell presence was assessed using 1% toluidine blue (Sigma-Aldrich, UK) with distilled water. This was performed for one minute with three washes in distilled water to remove excess stain.

2.4. Flame absorption spectrometry (FAAS) analysis of Mg and Mg–Ca alloy corrosion

Samples of culture medium collected each day were analysed for calcium and magnesium using a SOLAAR S Series AA spectrometer (Thermo Fisher Scientific, USA). An air acetylene mix was used for combustion. Signal correction was performed using a deuterium lamp. Burner height was optimised and held constant at 13.4 mm for calcium and 11.8 mm for magnesium. Cumulative values were plotted by adding the calculated ion content value of each day to the sum of the days prior to it. This was performed for magnesium and calcium correspondingly.

2.5. Analysis of precipitates formed during corrosion

Analysis of the crystals formed on the surface of the samples was analysed by field emission gun scanning electron microscopy (FEGSEM). Precipitates on the surface of the samples were ground to fine powder and allowed to dry for five days. The powder was then mounted on carbon disk topped stubs and gold sputter coated using a Q150T ES turbo pumped sputter coater (Quorum Technologies Ltd., East Sussex, UK). Analysis was performed on a 1530 VP FEGSEM (Carl Zeiss [Leo], Cambridge, UK).

X-Ray Powder Diffraction (XRD) was used to analyse surface crystals from Mg and Mg–Ca samples. The samples were scanned in a range between 10° and 90° using a D2 Phase X-ray diffraction tool (Bruker UK LTD, Coventry, UK).

2.6. Scanning electron microscope (SEM) imaging

Three iterations of Mg and Mg–Ca samples were prepared for imaging. These consisted of unaltered controls, exposed samples

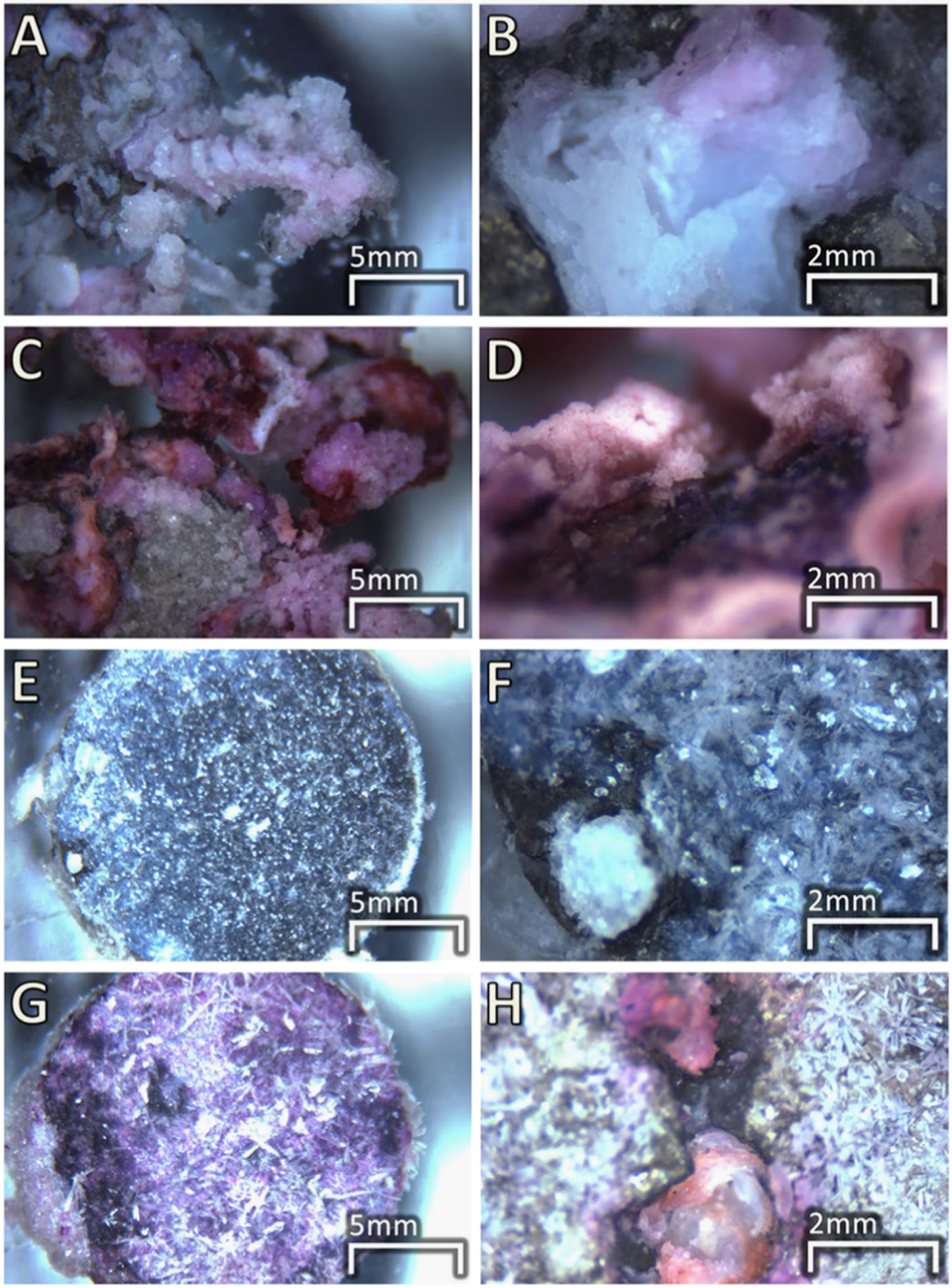

Fig. 1. Images of Mg and Mg–Ca alloy disks following 11 days cell culture: (A–D) Mg disks and (E–H) Mg–Ca disks. (C, D, G and H) Samples stained for calcium using Alizarin red.

demonstrating deposited crystals and samples with the top layer of crystal deposits removed. Samples were bonded to stubs using silver paste and sputter coated with a 70 nm layer of 80% gold/20% palladium using a SC7640 Sputter Coater (Quorum [Polaron], East Sussex, UK). Imaging was performed using a Stereo Scan 360 (Carl Zeiss [Leo/Cambridge], Cambridge, UK).

2.7. Corrosion rate calculation

Average corrosion rates were calculated according to the trend of cumulative Mg release using the following equation:

$$R = \frac{\alpha t + \beta}{2\pi r^2 + 2\pi r h} \quad (1)$$

where R is the corrosion rate, t is the duration of corrosion in days; $t=365$ for annual corrosion rate, r is the radius average of samples ($n=3$), h is the height average of samples ($n=3$) and α and β are constants from the linear trend of cumulative Mg release. The values of α and β are shown in Fig. 5E and F in the form $y=\alpha x+\beta$.

3. Results

3.1. Macroscopic observations

Imaging was performed using a macroscope at the end of the culture period. Resulting images are shown in Fig. 1. Culture was performed in serum containing medium with cells. The magnesium disks (A–D) demonstrated a significant structural change, ranging from small surface erosional pits (B) to large outgrowths of deposited crystal structures (A). This structural damage eventually resulted in an overall catastrophic failure of the sample structure with multiple fracture points separating the disk into several smaller structures(C). The magnesium with 1% calcium disks (E–H) demonstrated lessened structural change when compared to the magnesium disks. Most of the surface remained constant with the presence of small crystal deposits (E and G). A small number of surface erosional pits were observed each with the presence of larger crystalline structures (F and H). Overall structural integrity remained throughout the culture period due to the much slower corrosion.

Both magnesium and magnesium with 1% calcium disks were stained using an Alizarin red calcium stain. This demonstrated an even distribution of red stain throughout both samples (C, D, G and H) with the magnesium demonstrating a slightly more intense red.

3.2. Scanning electron microscope (SEM) imaging

Images obtained *via* SEM are shown in Fig. 2. These clearly demonstrate the presence of crystals on the surface of both the Mg and Mg–Ca samples. Whilst crystalline structure is very similar between the Mg and Mg–Ca samples, subtle differences

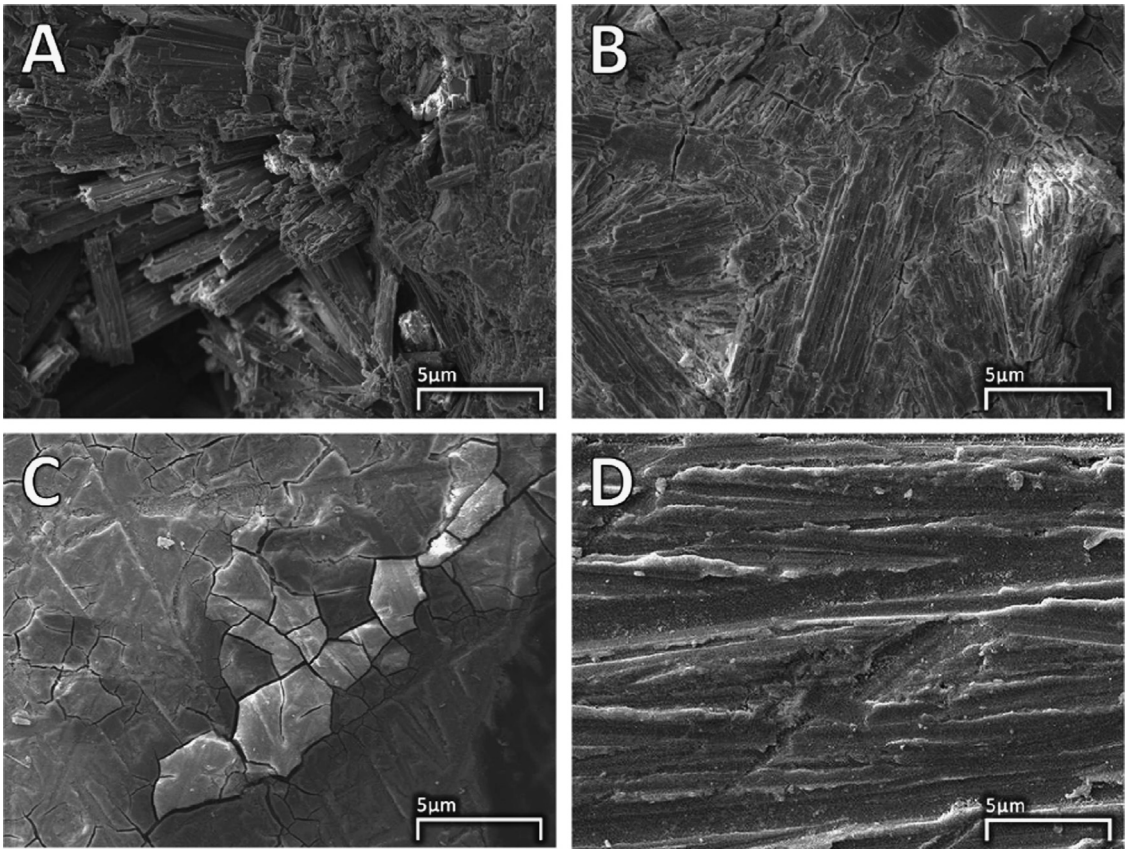

Fig. 2. SEM images demonstrate the coarser crystalline structure of the Mg (A) when compared to that of the Mg–Ca (B). Micro-fractures are present on the surface of the Mg sample (C) when the crystalline layer is removed. Conversely, the structure of the Mg–Ca (D) demonstrates less on the way of micro-fractures once the crystalline layer has been removed.

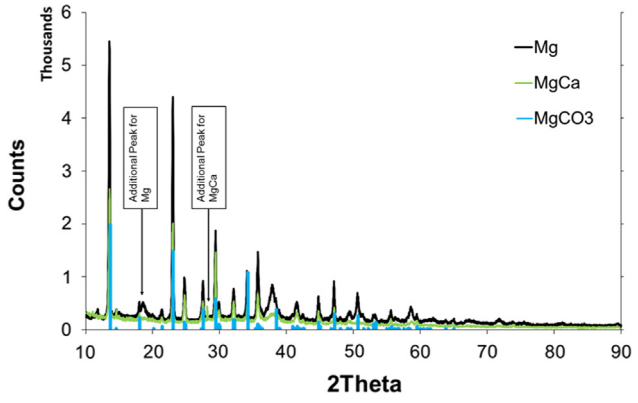

Fig. 3. XRD data showing the close match between both Mg and Mg–Ca and the XRD profile for $MgCO_3 \cdot 3H_2O$. Data based on corrosion without the presence of cells.

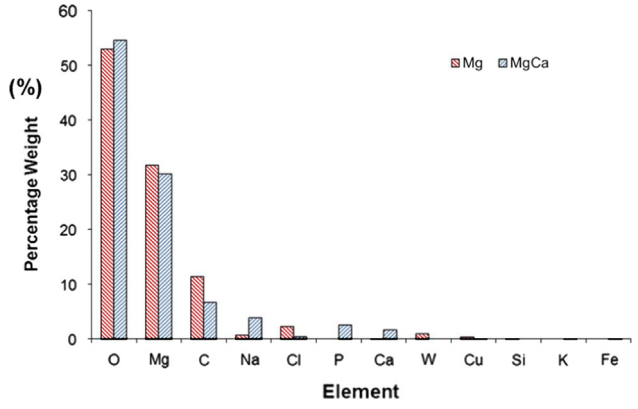

Fig. 4. FEGSEM data demonstrating the difference in composition between the Mg and Mg–Ca crystals (W, Cu, Si, K and Fe were discounted due to negligible presence). Data based on corrosion without the presence of cells.

in the characteristics of the crystal formations are visible. The Mg samples demonstrate a dynamic and porous structure. Conversely, the Mg–Ca crystals present a more compact and planar formation. Crystalline debris was present on both Mg and Mg–Ca samples at higher magnification. Following removal of the top layer of crystals from the samples, cracks in main metallic structure were exposed.

3.3. Analysis of precipitates formed during corrosion

The result from the XRD analysis shows that crystalline phase of magnesium carbonate ($MgCO_3$) was present on the surface of both the Mg and Mg–Ca samples. The peaks shown by XRD pattern correlated strongly with the specific peaks of $MgCO_3$, apart from only one additional peak for each sample (Fig. 3).

The results from the FEGSEM analysis demonstrate that the three most abundant elements by weight were oxygen, magnesium and carbon (Fig. 4). This is concurrent with the crystalline phase of magnesium carbonate demonstrated by the XRD data, however it should be noted that the FEGSEM also detected phosphate. In addition to this, sodium, potassium and calcium as well as trace elements were found to be present in the Mg–Ca precipitate. The calcium content in the Mg–Ca precipitate was measured at 1.63 wt%, which is higher than the stated 1 wt% of calcium in the alloy. In the crystal precipitates obtained from Mg samples the presence of chlorine was detected at 2.24 wt%.

3.4. Corrosion of Mg and Mg–Ca alloy

Magnesium and calcium ions released over the incubation process with or without the cell presence was analysed using FAAS. Fig. 5 shows that the calcium concentration is consistently lower than those in the control for both Mg and Mg–Ca and dramatic variation between the two types of metal samples was observed without the cell presence. The magnesium concentration was kept consistent at a much higher level, ranging from 40 to 80 mM for both Mg and Mg–Ca samples. Cumulative magnesium showed a constant release of magnesium ions from both Mg and Mg–Ca alloys throughout the culture. This trend is apparent both in concurrent culture with and without cells, *albeit* at a marginally increased rate with cellular presence. The average corrosion rates calculated according to the trend are listed in Table 1.

3.5. Cell presence

When comparing the control (A) to the Mg–Ca samples, Fig. 6 reveals that, cells cultured in the presence of Mg–Ca (B) did not proliferate and only a few cells could be visualised on the base of the well when compared to the control (A). Similarly, few cells were seen to be attached to the crystal precipitate on the surface of the Mg–Ca sample at the end of the culture. No cells could be observed in culture with the presence of Mg.

4. Discussion

During the 11 days culture period, magnesium concentration was consistently kept at higher level in a range of 40–80 mM for both Mg and Mg–Ca samples. At the end of the culture, the level of corrosion was found to be higher in the Mg samples demonstrating an increased presence of crystalline structures of Mg ionic compounds as indicated by strong Alizarin red staining. However, the Mg–Ca samples, demonstrate much lower levels of corrosion as well as a thinner, visible passivation layer of crystals on the surface. Corrosion rate of Mg is dependent upon solution loading capacity of magnesium ions as well as pH. As has been previously suggested [26], both pH increase and high solution concentrations of Mg stabilise the metallic surface, thus slowing the corrosion. However with medium change these factors are lowered and the surface becomes less stable and corrosion is resumed as evidenced by the linear cumulative release of Mg ions for both Mg and Mg–Ca (Fig. 5). These results suggest that corrosion behaviour of Mg alloys depends not only on the alloy but also on the rate of removal of corrosion products from the implantation site. Other studies have also reported different corrosion rates and behaviour based on the location of the

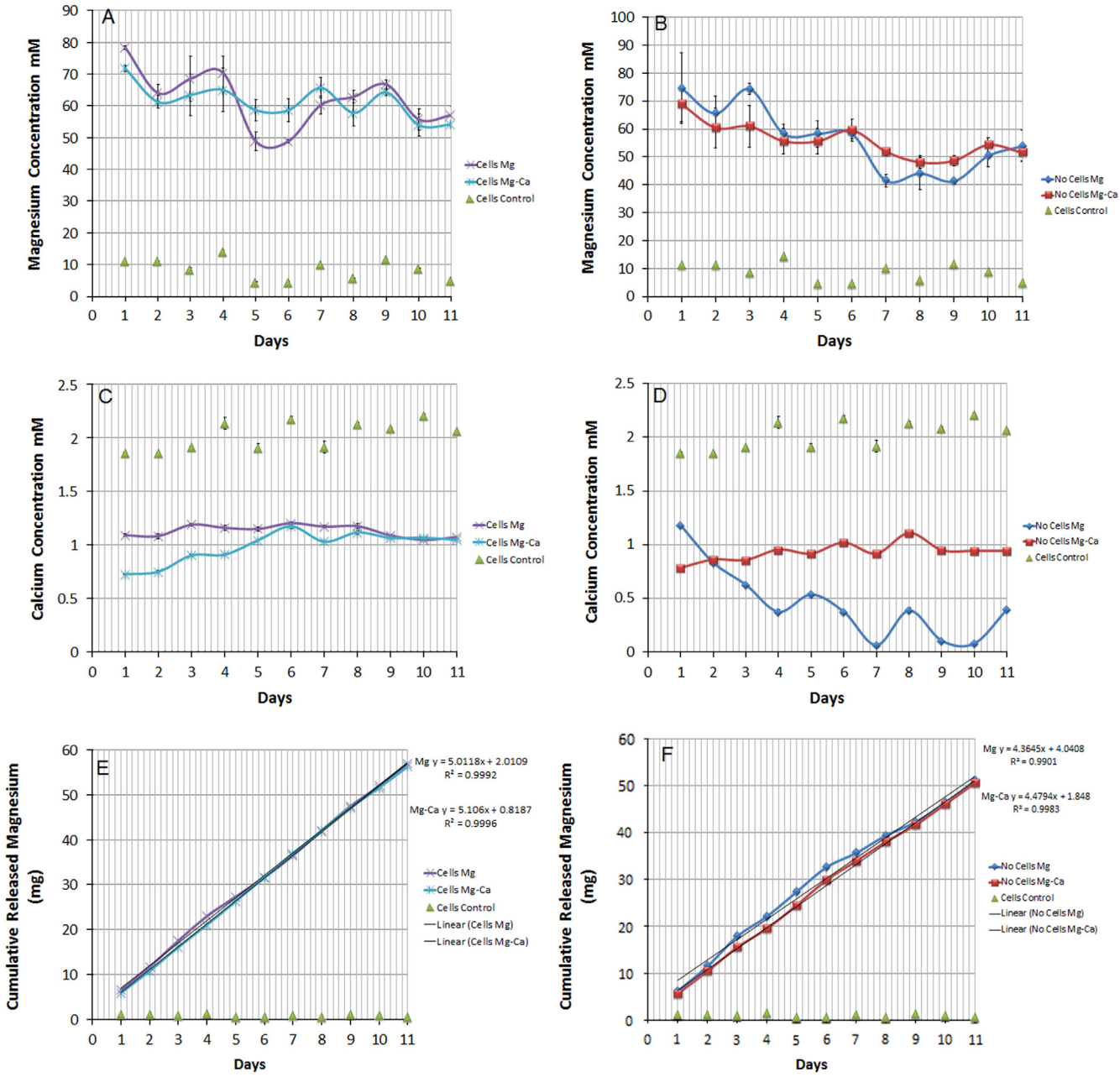

Fig. 5. (A–D) Measurements of calcium and magnesium concentration in conditioned medium with and without cell presence. Also cumulative magnesium release (E and F) are calculated indirectly through leaching loss, taking into account constant concentration increase each day as media was replaced.

magnesium alloy, with implants located near blood vessels having higher corrosion rates compared to those located in cortical bone [18,27]. Therefore, when designing magnesium-based implants it is important to consider not only the composition of the alloy but also the location and environment of the implantation.

The phase of magnesium found in the current study was magnesium carbonate hydrate ($MgCO_3$) as evidenced by XRD of crystals collected from Mg and Mg–Ca samples (Fig. 3). However in the previous study using the same alloy (Mg–Ca), the main corrosion product that was detected was magnesium hydroxide $Mg(OH)_2$. The major difference between the conditions of *in vitro* corrosion in the current study and previous research [24] is that cell culture medium saturated with CO_2 was applied instead of simulated body fluid (SBF). It seems that the presence of bicarbonate ions in the medium have resulted in the formation of $MgCO_3$ crystals rather than Mg

Table 1
Average corrosion rates calculated according to the trend of cumulative Mg release.

	Without the presence of cells (mg/year/mm^2)	With the presence of cells (mg/year/mm^2)
Mg	3.84	4.40
Mg–Ca alloy	2.80	3.18

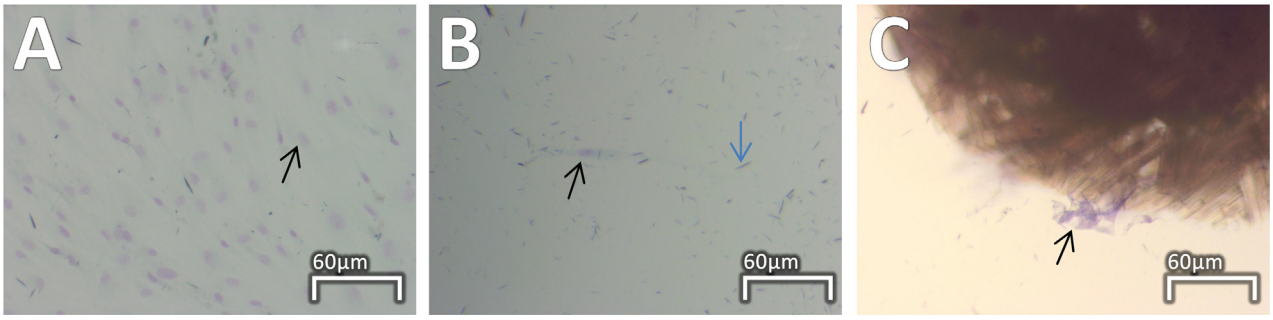

Fig. 6. Toluidine blue staining of cells on the tissue culture treated plastic control (A), with the presence of Mg–Ca (B) and adhering to the crystals precipitated on the surface of Mg–Ca (C). Black arrow indicates cell nucleus, blue arrow indicates precipitates formed during degradation.

$(OH)_2$, attributing to the following reaction:

$$Mg^{2+} + 2HCO_3^- \rightarrow MgCO_3 + CO_2 + H_2O$$

The observation of $MgCO_3$ crystals in the current study was consistent with those reported by Willumeit [28] and supported the hypothesis that $MgCO_3$, rather than $Mg(OH)_2$, would be the dominant component of the corrosion layer when corrosion solution was saturated with Mg^{2+} and HCO_3^- due to the presence of excessive Mg alloy and of continuous supply of CO_2 [28,29].

Within this study, a liner trend of Mg release was observed, indicating the corrosion process of Mg and Mg–Ca alloy. The corrosion product was removed with partial medium replacement after every 24 h to simulate the local removal of the corrosion products *in-vivo* environment. Furthermore the *in vitro* Mg–Ca corrosion rate calculated from the trend of corrosion in the current study, 2.81 and 3.2 mg/mm^2/year with and without the presence of cells respectively, closely relate to the rate (2.28 ± 0.13 mg/mm^2/year) observed *in vivo* [24]. The previous [24] study reported a higher *in vitro* corrosion rate (10.49 mg/mm^2/year); this difference can be attributed to the conditions of the corrosion test. SBF has high concentration of chloride ions (147.8 mM) compared to DMEM (109.5 mM) and the presence of chlorides ions in corrosive media results in the transformation of $Mg(OH)_2$ to highly soluble $MgCl_2$ making magnesium more susceptible to corrosion attack [30]. It has also been reported that the presence or absence of proteins alter the corrosion behaviour of Mg alloys, with both promoting and inhibiting effects reported [31,32]. In this study the presence of hMSCs resulted in a marginal increase in corrosion rate, further study is needed to confirm this and to understand the role played by cells in Mg corrosion.

During the corrosion process, elements are lost from the material and corrosion products precipitate on the surface of the metal. Fig. 5 shows that the amount of calcium ion released into the media from Mg–Ca sample was lower compared to the concentration of Ca ions in the control sample. Furthermore FEGSEM detected the presence of Ca and P on the surface of Mg–Ca sample (Fig. 4). It is likely that the formation of calcium phosphate salts (CaP) depleted the media ion content in favour of CaP formation. Although the calcium and phosphate content in the precipitates on Mg–Ca was measured at 1.63 wt% and 2.53 wt% respectively, no hydroxyapatite (HA) pattern was shown in XRD. Hence, there was not enough data to support that Ca and P presence in the precipitates on Mg–Ca sample surface was crystalline HA, however the presence of amorphous HA in the precipitates should not be excluded. Apart from the $MgCO_3$ XRD patterns, additional peaks were also observed; further research is needed to understand the origin of these peaks in precipitates formed at Mg–Ca surface.

The presence of magnesium may have a profound influence on cells. Previously it has been found that cells were able to survive in the presence of magnesium both in *in vitro* and *in vivo* conditions [14,16,20,23,24,33]. Magnesium and calcium are well tolerated by the body; they are essential minerals that play important roles in the body. Furthermore the release of Mg ions has been shown to enhance osteoblast activity [34]. However, in the previous study by Li [24], it had been noted that whilst osteoblasts survived in the region of the magnesium pin, as it degraded, no regeneration occurred. This may suggest that the bone tissue regeneration process could be affected by the limited number of bone forming cells at the implantation site.

We found that in the presence of Mg, no cells were able to survive either attached to tissue culture plastic or to the metallic samples themselves. Conversely, Mg–Ca alloy was found to support hMSC adhesion both in the surrounding environment, as well as directly on crystals precipitated on metallic sample (Fig. 6). It was however noted that the overall cell presence was low and failed to proliferate through the culture period. Another study [19] also showed that the culture of cells in direct contact with Mg alloy resulted in areas of minimal cell growth and no cell attachment was observed. Furthermore cell viability tends to be higher with indirect assays compared to direct cytocompatability tests [19,23,25]. However it is possible to encourage stem cell-initiated bone regeneration activities at implantation site since attachment and even proliferation have been reported when cells were cultured with Mg alloy of controlled corrosion rate [14,23]. It has also been suggested that the evolution of hydrogen from the surface of the sample might be responsible for disrupting cell adhesion and cell growth [23]. Therefore, in future studies it is important to understand the effect of Mg-alloy implants on local stem cell populations and progenitor cells in order to maximise the regeneration capability of these cells.

5. Conclusion

In general, *in vitro* study of corrosion of Mg–Ca in biologically-simulated environment using cell culture medium with the presence of hMSC demonstrated close resemblances to *in vivo* corrosion. Although *in vitro* corrosion of Mg–Ca revealed slow corrosion rate and no immediate cytotoxicity effects to hMSCs, its corrosion rate was still too high to achieve normal stem cell growth when cells and alloys were cultured *in vitro* in direct contact.

Acknowledgements

We greatly appreciate technical assistance provided by Trevor Brown (atomic absorption spectroscopy), Deepak Kanda Kumar (providing cells for examination), Dr. Keith Yendall (FEGSEM, XRD) and Shaun Fowler (SEM imaging). Funding for this research was provided by an Engineering and Physical Sciences Research Council (Grant no. EPF500491/1) Doctoral Training Centre (R.H and D.M.) and EPSRC vocational bursary (S.L.).

References

[1] F. Witte, V. Kaese, H. Haferkamp, E. Switzer, A. Meyer-Lindenberg, C.J. Wirth, et al., Biomaterials 26 (2005) 3557–3563.
[2] N.T. Kirkland, N. Birbilis, M.P. Staiger, Acta Biomater. 8 (2012) 925–936.
[3] M.L. Oyen, V.L. Ferguson, A.K. Bembey, A.J. Bushby, A. Boyde, J. Biomech. 41 (2008) 2585–2588.
[4] J.Y. Rho, R.B. Ashman, C.H. Turner, J. Biomech. 26 (1993) 111–119.
[5] C. Castellani, R.A. Lindtner, P. Hausbrandt, E. Tschegg, S.E. Stanzl-Tschegg, G. Zanoni, et al., Acta Biomater. 7 (2011) 432–440.
[6] R.D. Grubbs, M.E. Maguire, Magnesium 6 (1987) 113–127.
[7] K.W. Beyenbach, Magnes. Trace Elem. 9 (1990) 233–254.
[8] N.L. Saris, E. Mervaala, H. Karppanen, J.A. Khawaja, A. Lewenstam, Clin. Chim. Acta 294 (2000) 1–26.
[9] W.E. Wacker, A.F. Parisi, N. Engl. J. Med. 278 (1968) 772–776.
[10] P.W. Flatman, Annu. Rev. Physiol. 53 (1991) 259–271.
[11] A.M. Romani, A. Scarpa, Front. Biosci. 5 (2000) D720–D734.
[12] Z.S. Agus, M. Morad, Annu. Rev. Physiol. 53 (1991) 299–307.
[13] M.M. Belluci, T. Schoenmaker, C. Rossa-Junior, S.R. Orrico, T.J. de Vries, V. Everts, J. Nutr. Biochem. 24 (2013) 1488–1498.
[14] D. Hong, P. Saha, D.T. Chou, B. Lee, B.E. Collins, Z. Tan, et al., Acta Biomater. 9 (2013) 8534–8547.
[15] I. Johnson, H. Liu, PLoS One 8 (2013) e65603.
[16] R.G. Guan, I. Johnson, T. Cui, T. Zhao, Z.Y. Zhao, X. Li, et al., J. Biomed. Mater. Res. A 100 (2012) 999–1015.
[17] H. Liu, J. Biomed. Mater. Res. A 99 (2011) 249–260.
[18] T.A. Huehnerschulte, J. Reifenrath, B. von Rechenberg, D. Dziuba, J.M. Seitz, D. Bormann, et al., Biomed. Eng. Online 11 (2012) 14(14-925X-11-14).
[19] J.D. Cao, P. Martens, K.J. Laws, P. Boughton, M. Ferry, J. Biomed. Mater. Res. B: Appl. Biomater. 101 (2013) 43–49.
[20] M.E. Iskandar, A. Aslani, H. Liu, J. Biomed. Mater. Res. A 101 (2013) 2340–2354.
[21] W. Lu, W. Duan, Y. Guo, C. Ning, J. Biomater. Appl. 26 (2012) 637–650.
[22] B. Wang, J. Gao, L. Wang, S. Zhu, S. Guan, Mater. Lett. 70 (2012) 174–176.
[23] X. Gu, Y. Zheng, S. Zhong, T. Xi, J. Wang, W. Wang, Biomaterials 31 (2010) 1093–1103.
[24] Z. Li, X. Gu, S. Lou, Y. Zheng, Biomaterials 29 (2008) 1329–1344.
[25] X.N. Gu, W.R. Zhou, Y.F. Zheng, Y. Cheng, S.C. Wei, S.P. Zhong, et al., Acta Biomater. 6 (2010) 4605–4613.
[26] J.E. Gray-Munro, C. Seguin, M. Strong, J. Biomed. Mater. Res. A 91 (2009) 221–230.
[27] N. Erdmann, N. Angrisani, J. Reifenrath, A. Lucas, F. Thorey, D. Bormann, et al., Acta Biomater. 7 (2011) 1421–1428.
[28] R. Willumeit, J. Fischer, F. Feyerabend, N. Hort, U. Bismayer, S. Heidrich, et al., Acta Biomater. 7 (2011) 2704–2715.
[29] H. Waizy, J. Seitz, J. Reifenrath, A. Weizbauer, F. Bach, A. Meyer-Lindenberg, et al., J. Mater. Sci. 48 (2013) 39–50.
[30] L. Li, J. Gao, Y. Wang, Surf. Coat. Technol. 185 (2004) 92–98.
[31] L. Yang, N. Hort, R. Willumeit, F. Feyerabend, Corros. Eng. Sci. Technol. 47 (2012) 335–339.
[32] X.N. Gu, Y.F. Zheng, L.J. Chen, Biomed. Mater 4 (2009) Article no. 065011, http://dx.doi.org/10.1088/1748-6041/4/6/065011(Epub).
[33] J.D. Cao, N.T. Kirkland, K.J. Laws, N. Birbilis, M. Ferry, Acta Biomater. 8 (2012) 2375–2383.
[34] H. Zreiqat, C.R. Howlett, A. Zannettino, P. Evans, G. Schulze-Tanzil, C. Knabe, et al., J. Biomed. Mater. Res. 62 (2002) 175–184.